

SUPPLEMENTAL Information

**pHTomato: A genetically-encoded indicator that enables multiplex
interrogation of synaptic activity**

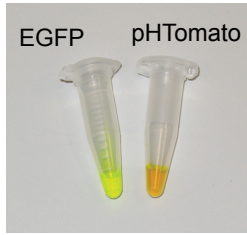
Yulong Li¹, Richard W. Tsien^{1,2}

1.Department of Molecular and Cellular Physiology
Stanford University School of Medicine
279 Campus Dr., Stanford, CA 94305, USA

2.NYU Neuroscience Institute and Department of Physiology and Neuroscience, New York
University, New York, NY 10016, USA

Sup_Fig-1 (Li)

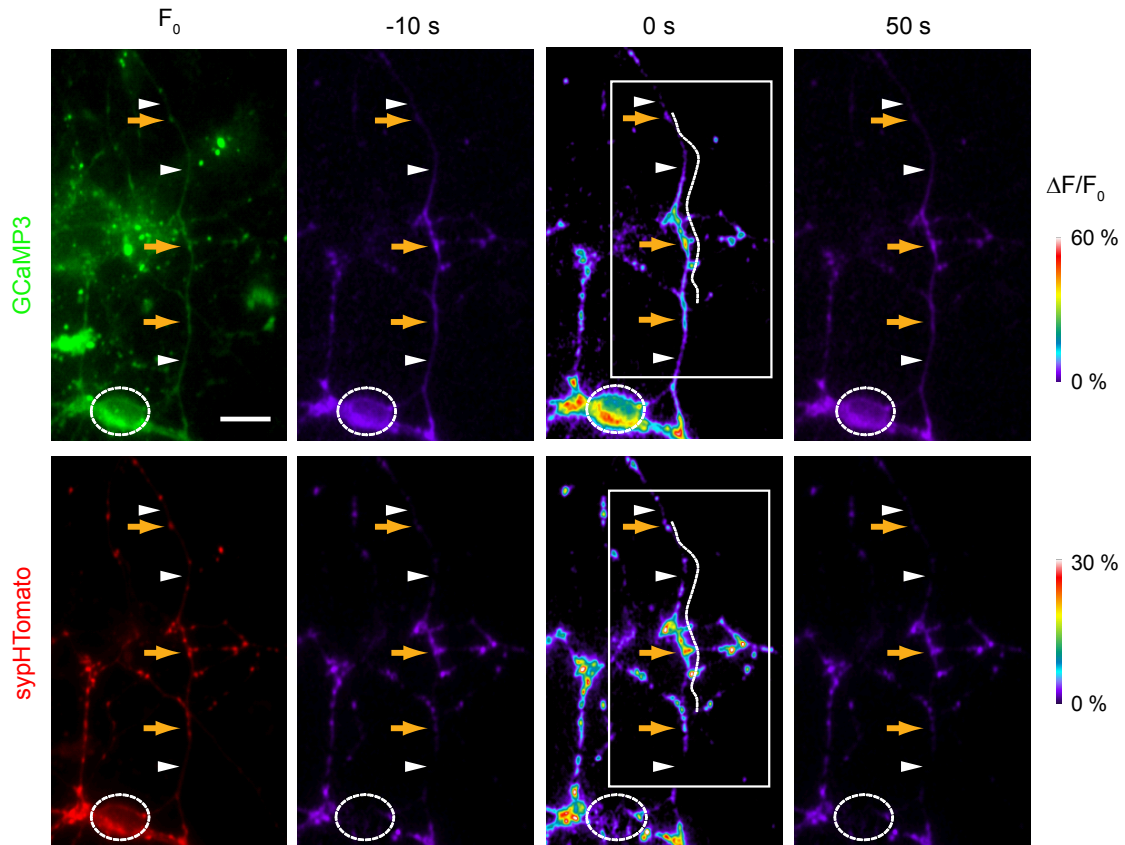
a



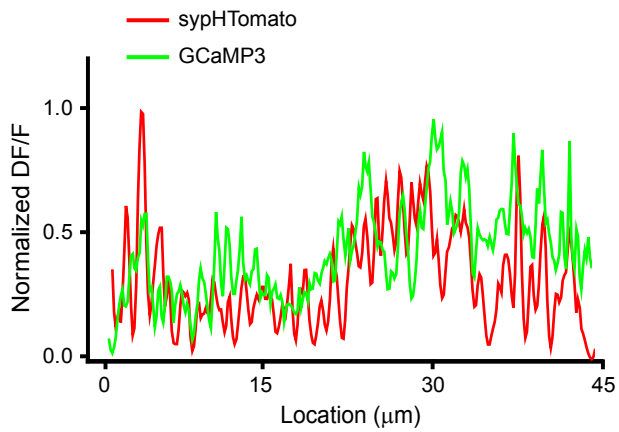
b

	Quantum yield	Extinction coefficient (M ⁻¹ cm ⁻¹)
pHTomato	0.68	70500
EGFP	0.60	55000

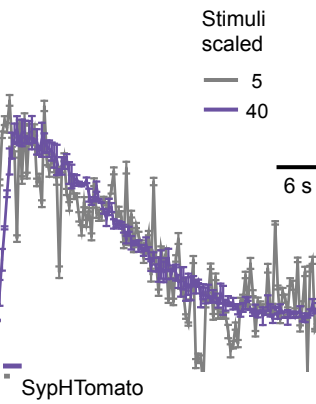
c



d

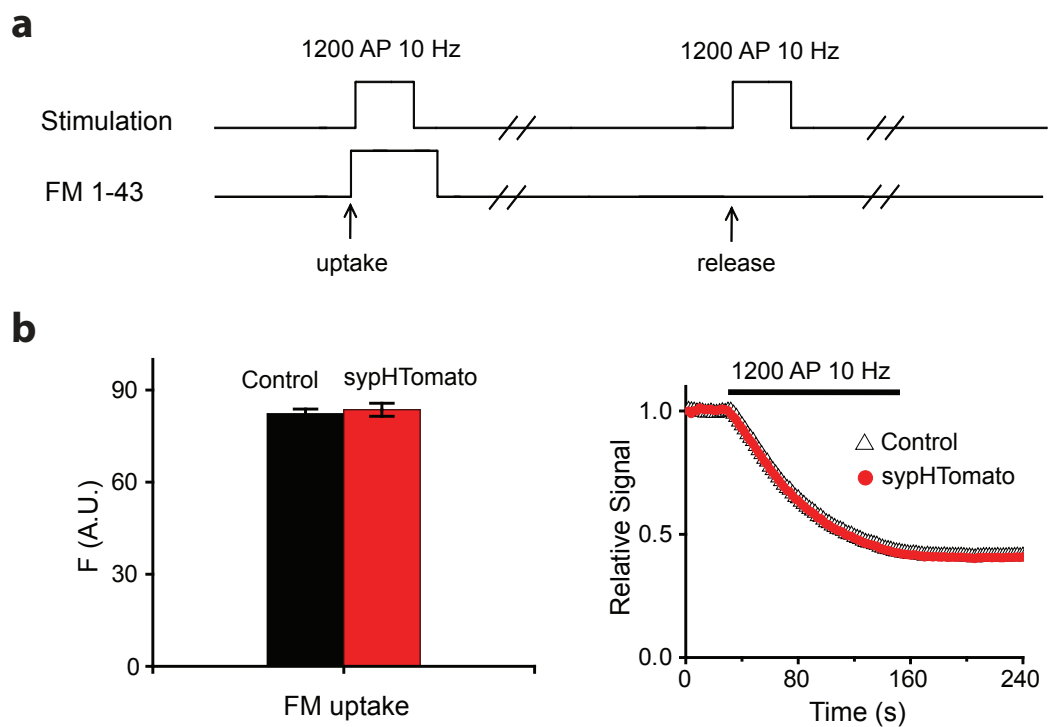


e



Supplemental Figure 1. pHTomato properties and dual color imaging of $[Ca^{2+}]_{cytosolic}$ and vesicle fusion from the same neuron. (a) Purified recombinant pHTomato and EGFP fluorescent proteins, shown in visible light. (b) Properties of pHTomato in comparison to EGFP. Extinction coefficients were measured by the alkali denaturing method. Value for EGFP from reference³⁸. (c) Time-lapse recordings of dual color imaging of GCaMP3 signal (reporting $[Ca^{2+}]_{cytosolic}$) and SypHTomato signal (reflecting vesicle fusion), obtained by imaging in the same cultured hippocampal neuron. The peak responses from rectangular regions were shown in Fig. 2a. Oval indicates soma. Scale bar, 10 μ m. (d) Normalized fluorescence intensity plots ($\Delta F/F$) for the peak GCaMP3 and sypHTomato signals recorded along the axon (white line, Suppl. Fig. 1c) during the stimulation. (e) Comparison of the kinetics of sypHTomato responses to 5 and 40 stimuli at 20 Hz. No differences in the time course were observed between the two conditions ($\tau = 15.5 \pm 0.6$ s, $p > 0.1$)

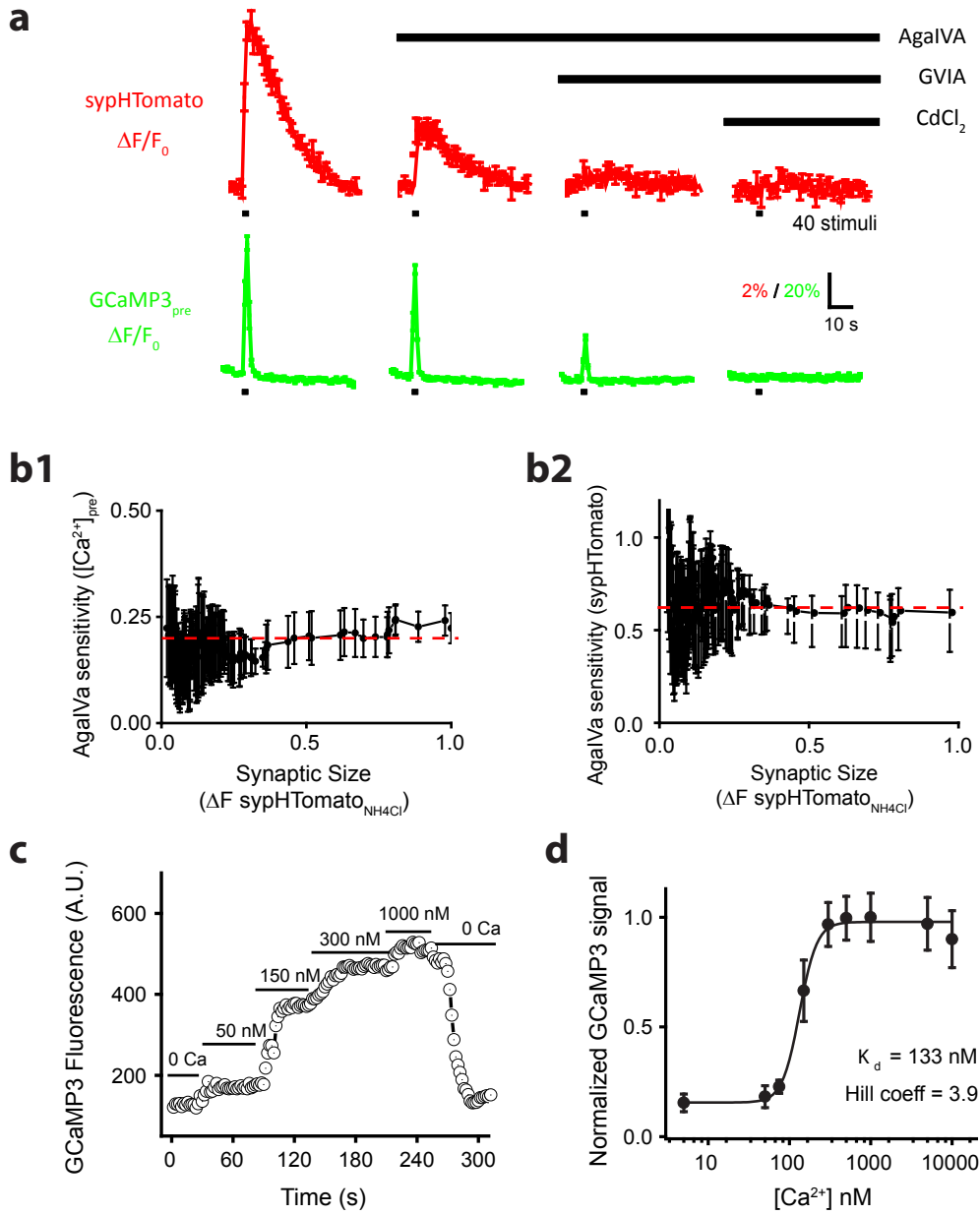
Sup_Fig-2 (Li)



Supplemental Figure 2. Effect of overexpression of sypHTomato on vesicular dynamics.

(a) The protocols for FM uptake and release to probe vesicular turnover. (b) sypHTomato expression causes no detectable change in FM dye uptake or release, indicating vesicular endocytosis and exocytosis are unperturbed. Data collected from 3 independent cultures loaded with FM 1-43 dye wherein control boutons (n=1112 total) and sypHTomato positive boutons (n=455 total) were compared.

Sup_Fig-3 (Li)

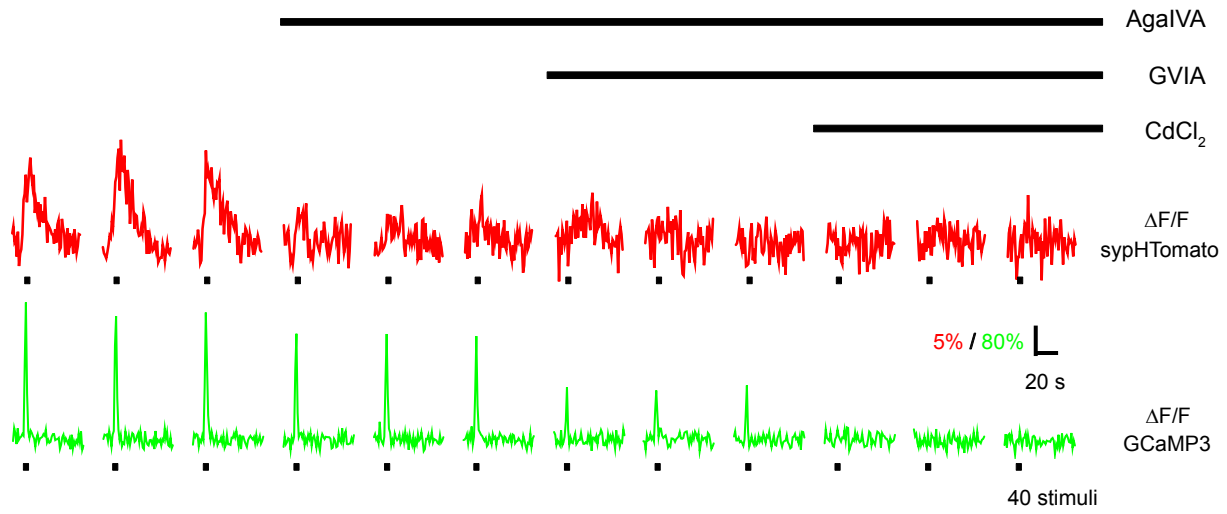


Supplemental Figure 3. GCaMP3 and sypHTomato allow for optical probing of multiple

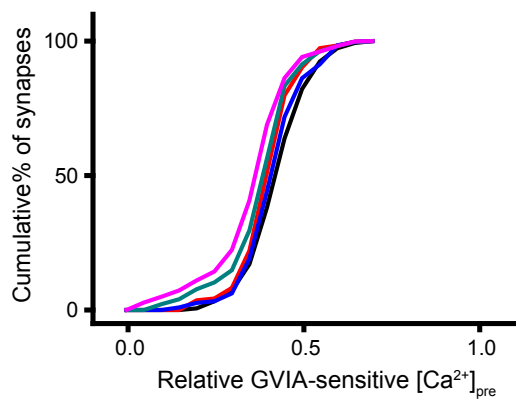
voltage-gated calcium channels at individual presynaptic release sites (a) Sequential and cumulative application of AgaIVA (1 μM), GVIA (1 μM) and CdCl_2 (100 μM) (black bars) inhibited Ca^{2+} signals (GCaMP3, $\Delta\text{F}/\text{F}$) and corresponding transmitter release (sypHTomato, $\Delta\text{F}/\text{F}$). (b) Heterogeneity of toxin sensitivity within individual boutons. Inhibition of volume averaged bouton $[\text{Ca}^{2+}]$ against synaptic size (probed by NH_4Cl challenge). b1, AgaIVA; b2: GVIA. Data from ~ 140 presynaptic boutons of the same neuron. Volume average $[\text{Ca}^{2+}]_{\text{pre}}$ was calculated based on the GCaMP3 signal and the corresponding calibration curve in (c,d). We calculate that, at worst, bulk calcium level could be underestimated by no more than 30%. (See methods) (c) *In situ* calibration of GCaMP3 in the presynaptic boutons, typically performed at the end of an experiment. Neurons were permeabilized with 10 μM ionomycin containing the indicated concentrations of Ca^{2+} (in nM). (d) *In situ* calibration curve for GCaMP3. Emission of GCaMP3 signal was normalized to the range produced by 1 μM Ca^{2+} and 0 Ca^{2+} . Data were least-squares fitted by a Hill function with Hill coefficient of ~ 4 . Error bars denote S.E.M.

Sup_Fig-4 (Li)

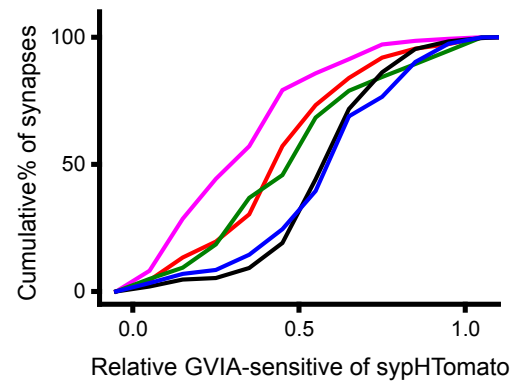
a



b

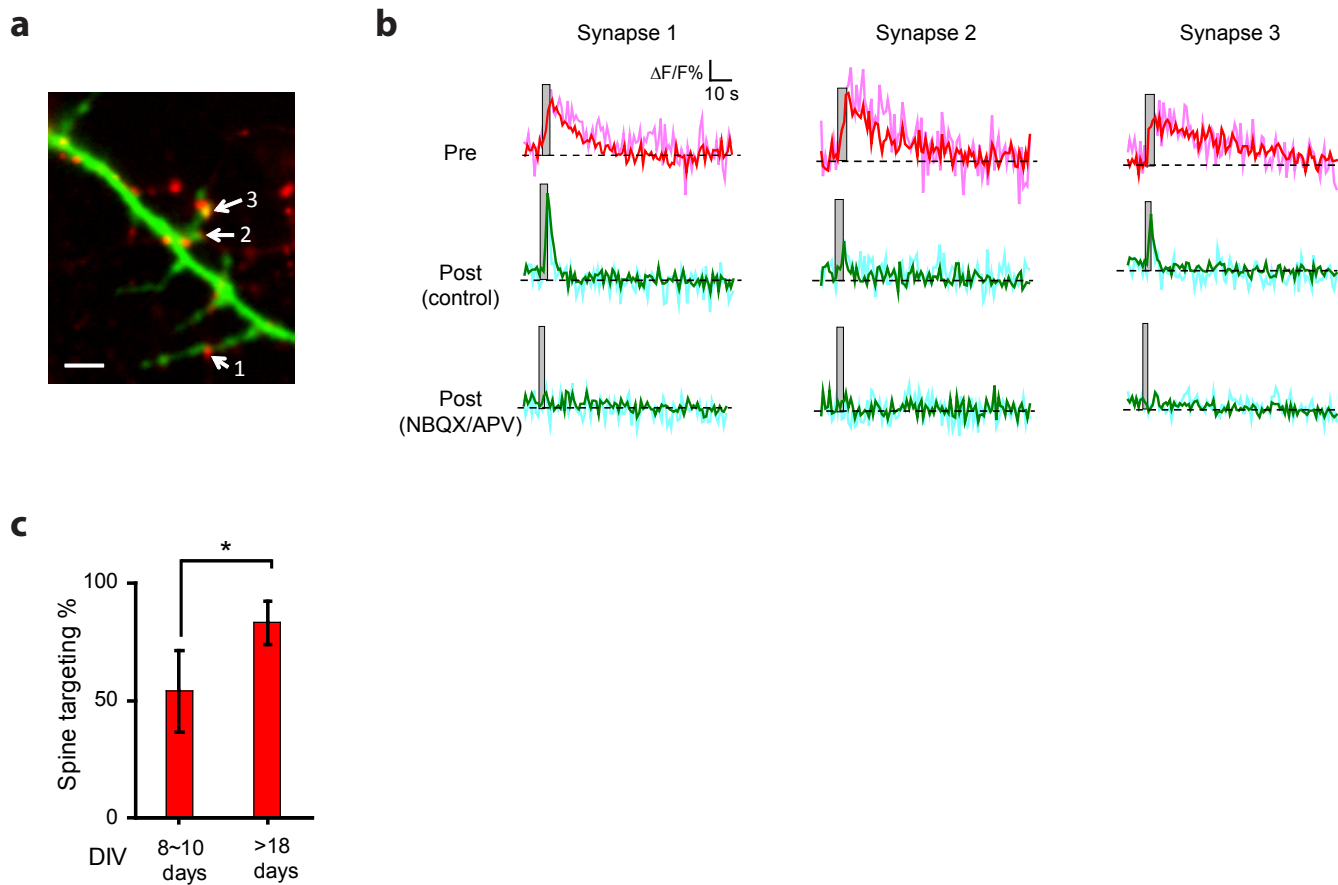


c



Supplemental Figure 4. (a) Traces from a single synapse show the trial-to-trial reliability of sypHTomato and GCaMP3 under various pharmacological conditions. Sequential and cumulative application of AgaIVA (1 μ M), GVIA (1 μ M) and CdCl₂ (100 μ M) (black bars) inhibited Ca²⁺ signals (GCaMP3, Δ F/F) and corresponding transmitter release (sypHTomato, Δ F/F). Data are obtained from the same neurons shown in Suppl. Fig. 3. (b,c). Heterogeneity of toxin sensitivity for N type calcium channel GVIA across individual boutons. Cumulative inhibition of volume average [Ca²⁺] (b) or sypHTomato (c) by GVIA for each bouton was plotted. N=5 neurons.

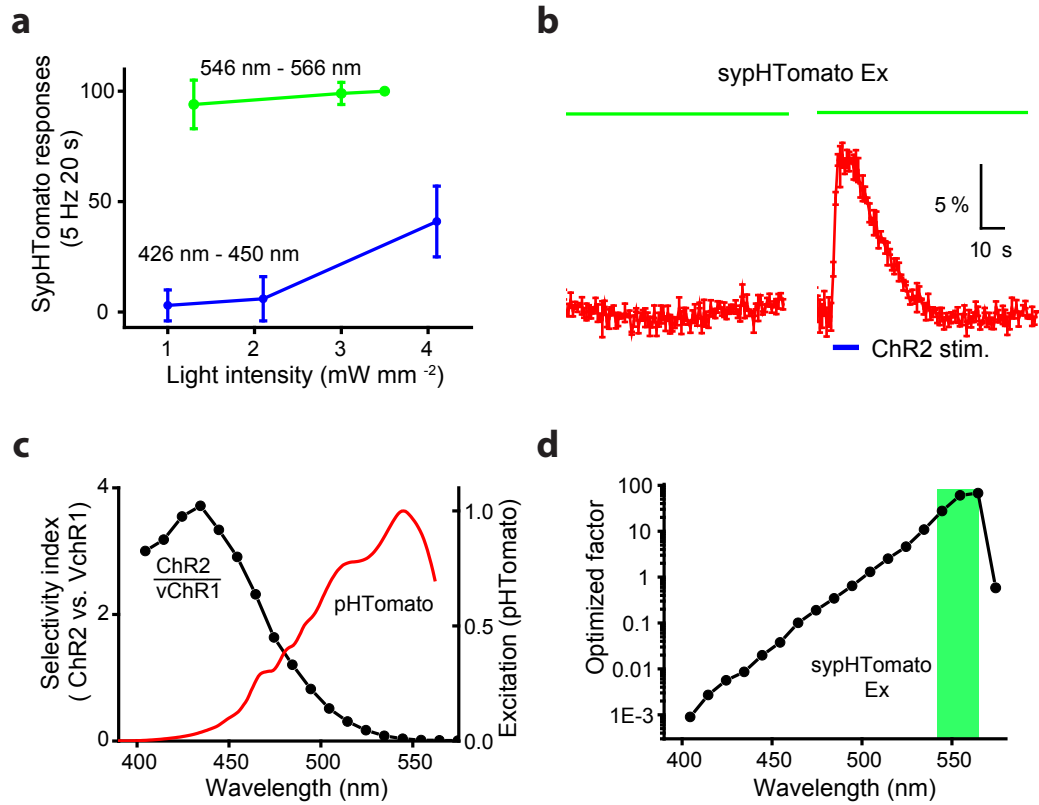
Sup_Fig-5 (Li)



Supplemental Figure 5. Trial-to-trial reliability of sypHTomato and GCaMP3 signals from connected pair of neurons.

(a) A dual color imaging showing a connected pair of neurons in which the presynaptic neuron expressed sypHTomato and postsynaptic neuron expressed GCaMP3. (b) Traces from selected ROIs, showing single trial responses (faint traces) and averages of five trials responses (bold traces) under various pharmacological conditions, Box indicates stimulation with 40 shocks at 20 Hz. A cocktail of NBQX(10 μ M) and APV (50 μ M) completely blocked the postsynaptic GCaMP3 responses. Scale bar, 2 μ m. (c) Quantification of spine targeting at different developmental ages. Putative postsynaptic structures directly contacting sypHTomato-labeled varicosities were classified into protrusive spine-like structures and non-protrusive dendrites. Mature neurons(>18 DIV, n= 5 neurons, 34 synapses) displayed a greater degree of spine targeting (73% \pm 7%) than developing synapses (DIV 8-10 days, 53% \pm 11%, n =41 synapses, 6 neurons). P<0.05, t test.

Sup_Fig-6 (Li)



Supplemental Figure 6. Optimal light intensity and spectral windows for photostimulation and optical imaging. (a) Minimal cross-activation of vChR1 by low intensity blue light (426-450 nm, $<2\text{mW/mm}^2$); green light (546-566nm), from 1 to 4 mW/mm^2 , consistently activated vChR1. (b) Tests of ChR2 in combination with sypHTomato as proof-of-principle of all-optical yet independent monitoring and stimulation. Left, interrogation of sypHTomato with Green light (546 -566nm) excitation alone without activation of ChR2-driven vesicular turnover. . Right, positive control with blue light (457-482 nm), showing robust ChR2-driven sypHTomato transient (right). Neurons were co-transfected with ChR2 and sypHTomato and imaged in an external solution containing 5mM Ca and 0 mM Mg, a condition optimized for signal detection of sypHTomato. N=231 boutons. Data are averaged of 3 trials. Error bar, SEM. (c) Theoretical selectivity index computed is the ratio of the action spectra for ChR2 and vChR1. The peak at 430 nm is optimal for selective activation of ChR2 with minimal activation of vChR1. Excitation spectrum of pHTomato shows minimal excitation at 430 nm. (d) Optimal conditions for using the same spectral window to stimulate vChR1 and interrogate sypHTomato. “Optimal factor” $f_{\text{opt}} = \text{Ex}_{\text{pHTomato}} * A_{\text{vChR1}} / A_{\text{ChR2}}$, where $\text{Ex}_{\text{pHTomato}}$ represents the excitation spectrum for pHTomato and A_{vChR1} and A_{ChR2} are action spectra for ChR2 and vChR1 respectively. Green bar indicates the band where the highest performance is expected.